LUND UNIVERSITY

Resistivity monitoring for leakage and internal erosion detection at Hallby embankment dam

Sjodahl, P.; Dahlin, Torleif; Johansson, S.; Loke, M. H.

Published in:
Journal of Applied Geophysics

DOI:
10.1016/j.jappgeo.2008.07.003

2008

Link to publication

Citation for published version (APA):
Sjodahl, P., Dahlin, T., Johansson, S., & Loke, M. H. (2008). Resistivity monitoring for leakage and internal erosion detection at Hallby embankment dam. *Journal of Applied Geophysics*, *65*(3-4), 155-164. https://doi.org/10.1016/j.jappgeo.2008.07.003

Total number of authors:
4

General rights
Unless other specific re-use rights are stated the following general rights apply:
Copyright and moral rights for the publications made accessible in the public portal are retained by the authors and/or other copyright owners and it is a condition of accessing publications that users recognise and abide by the legal requirements associated with these rights.
• Users may download and print one copy of any publication from the public portal for the purpose of private study or research.
• You may not further distribute the material or use it for any profit-making activity or commercial gain
• You may freely distribute the URL identifying the publication in the public portal

Read more about Creative commons licenses: https://creativecommons.org/licenses/

Take down policy
If you believe that this document breaches copyright please contact us providing details, and we will remove access to the work immediately and investigate your claim.

LUND UNIVERSITY

PO Box 117
221 00 Lund
+46 46-222 00 00

Download date: 09. Sep. 2026

Journal of Applied Geophysics 65 (2008) 155–164

Contents lists available at ScienceDirect

Journal of Applied Geophysics

journal homepage: www.elsevier.com/locate/jappgeo

Resistivity monitoring for leakage and internal erosion detection at Hällby embankment dam

P. Sjödahl [a,*], T. Dahlin [b], S. Johansson [a], M.H. Loke [c]

[a] HydroResearch Sam Johansson AB, Box 1608, S-18316 Täby, Sweden
[b] Engineering Geology, Lund University, Box 118, S-221 00 Lund, Sweden
[c] School of Physics, Universiti Sains Malaysia, 11800 Penang, Malaysia

ARTICLE INFO

Article history:
Received 29 February 2008
Accepted 3 July 2008

Keywords:
Resistivity
Time-lapse inversion
Monitoring
Embankment dam
Leakage

ABSTRACT

Internal erosion is one of the major reasons for embankment dam failures. Despite this, the knowledge of the temporal development of internal erosion in full scale structures is limited. Detection of internal erosion is complicated using conventional methods, and new or improved methods are appreciated. Hällby was the first Swedish embankment to get a permanently installed monitoring system intended for resistivity measurements. Daily measurements started to take place already in late 1996, which make these long term monitoring data unique. This paper includes examples of long term time series from Hällby along with some evaluation and interpretation techniques used when analysing such monitoring data. Time-lapse inversion was used to focus the variation over time and suppress artefacts due to the resistivity structure. Seasonal resistivity variations inside the dam are obvious. Increasing long term resistivity has been noticed in a particular zone in the left embankment. This zone also exhibits larger seasonal variations relative to other parts of the dam, and the variations are increasing. The observations may relate to an ongoing internal erosion process in the dam. The long term change may be indicative of a change in material properties, and the large and increasing variations may reflect higher and increasing seepage levels. In the years 2004 to 2006 the dam was upgraded and the resistivity system reinstalled. The results indicate that resistivity monitoring may have a chance of detecting development of internal erosion at an early stage.
© 2008 Published by Elsevier B.V.

1. Introduction

Internal erosion is one of the major reasons for embankment dam failures. Resistivity monitoring may have the possibility of detecting internal erosion processes and anomalous seepage at an early stage before the safety of the dam is at stake. This is done by analysing and comparing the seasonal resistivity variation schemes in the reservoir and inside the dam body. The monitoring technique is essentially non-destructive, which is particularly important when working with embankment dams where drilling and other penetrating investigations are normally avoided. Other non-destructive methods, such as seismic methods and ground penetrating radar, have also been used in dam investigations but are less easily used for long term monitoring.

Electrical resistivity measurements have been used on numerous occasions for dam site investigations (e.g. Aina et al., 1996; Batayneh et al., 2001) and dam status control (e.g. Van Tuyen et al., 2000; Buselli and Lu, 2001; Panthulu et al., 2001; Voronkov et al., 2004; Cho and Yeom, 2007). As regards dam status control investigations, they typically include 2D resistivity profiling along the embankment crest or along the downstream toe, in order to locate anomalies. Other methods are frequently used to further investigate critical areas in more detail. This is a reasonable approach even though considerable deficiencies inside the dam are probably needed in most cases to make the method successful. Therefore, use of the method is usually called for only after some problem has already been reported. For example, it may be used to delineate known leakage areas, analyse erosion problems around observed sinkholes or detect areas with high pore water content in the downstream support fill.

Repeated measurements or full scale monitoring is a more powerful way, which better takes advantage of the methods true capabilities. The resistivity variations inside the dam are caused by the steady seepage of water from the reservoir, in that the seasonal resistivity variations of the reservoir water advances with the seepage water into the dam. Using the monitoring approach therefore adds the possibility to use the method for surveillance of critical dams and in favourable circumstances to analyse the patterns of seasonal resistivity variations to detect anomalous seepage through the dam body as suggested by Johansson and Dahlin (1996). The seasonal resistivity variation is mainly caused by the seasonal temperature variation. The variation of ion content, TDS (Total Dissolved Solids), in the water will

* Corresponding author. Tel.: +46 70 5564948; fax: +46 8 7564950.
E-mail addresses: pontus.sjodahl@hydroresearch.se (P. Sjödahl), torleif.dahlin@tg.lth.se (T. Dahlin), sam.johansson@hydroresearch.se (S. Johansson), mhloke@tm.net.my (M.H. Loke).

0926-9851/$ – see front matter © 2008 Published by Elsevier B.V.
doi:10.1016/j.jappgeo.2008.07.003

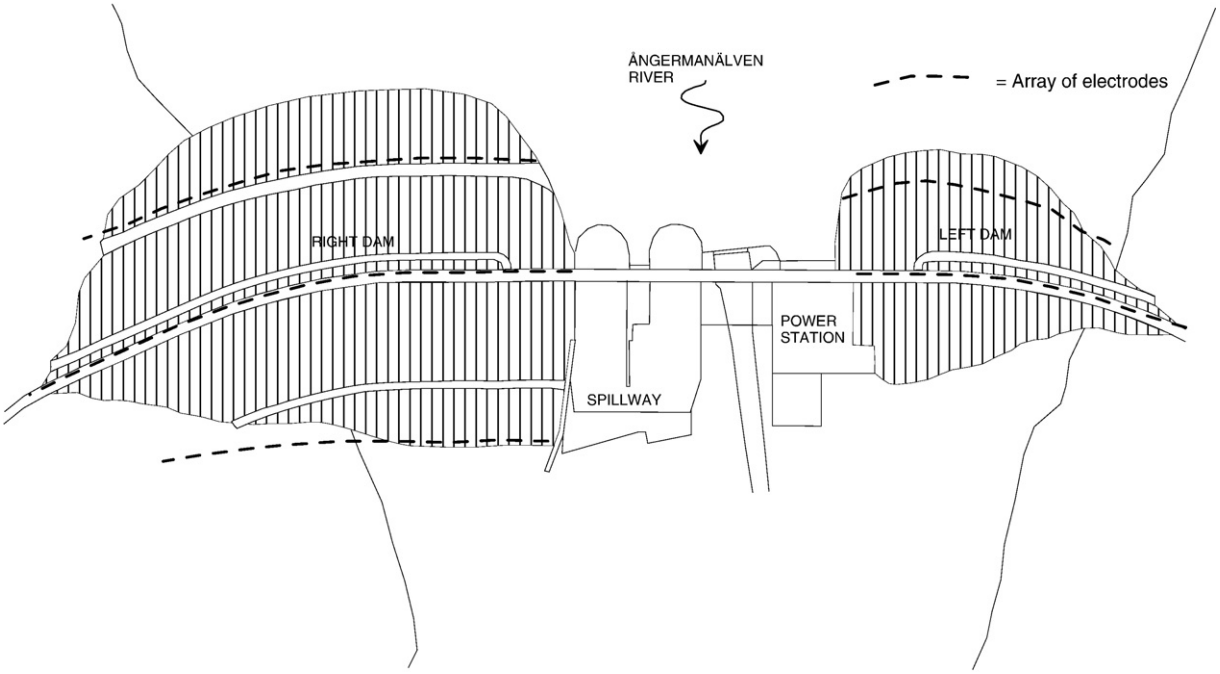

Fig. 1. Map over Hällby dam area. Principal location of electrodes marked out.

normally have a minor influence, but may also be of importance in some cases. The resistivity response inside the dam to these seasonal resistivity variation sources in the water depends on the seepage flow.

Considering the rapid development of instruments and evaluation techniques over the last few years this option is becoming more attractive. Repeated resistivity measurements have been used in several applications of groundwater studies (Barker and Moore, 1998), with other purposes than safety control of embankments, such as for instance mapping distribution of groundwater contaminants (e.g. Osiensky, 1995; Kayabali et al., 1998; Aristodemou and Thomas-Betts, 2000; Chambers et al., 2004; Depountis et al., 2005). Other areas include imaging changing moisture content distribution in engineered earthworks (Jackson et al., 2002), snowmelt infiltration (French and Binley, 2004) or monitoring of soil remediation works (LaBrecque et al., 1996) just to name a few. These applications are of high relevance for embankment dam monitoring studies, as many of the problems regarding monitoring techniques are similar. Of special importance, however, are studies made on similar material taking seasonal variations into account. Cuthbert et al. (2004) identified temperature effects in resistivity data from a glacial till in the UK and managed to fit it with a vertical conductive heat flow model using annual variation in surface air temperature as a boundary condition. Rein et al. (2004) identified natural daily and seasonal subsurface variations in apparent resistivity and recognised soil temperature and water temperature as the most significant factors next to water saturation, whereas natural variations due to water ion content had less impact on the results. Aaltonen (2001) carried out laboratory test on samples of different top layer mid-Swedish soils and found a considerable seasonal resistivity variation.

Work on monitoring of resistivity on dams with the purpose of dam safety surveillance is less common. In Sweden a few early tests using repeated resistivity measurements were carried out (Johansson and Dahlin, 1996) before a permanently installed system was designed at two dams in 1996 and 1999 (Johansson and Dahlin, 1998; Dahlin et al., 2001). Hällby was the first Swedish embankment to get a permanently installed monitoring system intended for resistivity measurements. Daily measurements started to take place already in late 1996. This paper includes examples of time series from Hällby along with some evaluation and interpretation techniques used when analysing long term monitoring data.

2. Site description

The embankment dam at Hällby is divided into a left and a right part (dam engineering terminology uses left and right looking in the direction of the river flow) by centrally placed power plant and

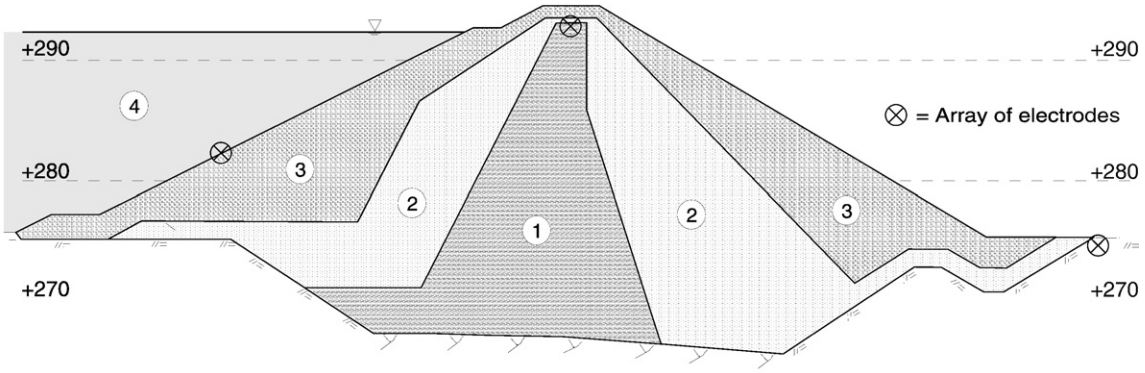

Fig. 2. Cross-section of Hällby dam. 1 Core, 2 filter, 3 support rockfill (upstream and downstream), 4 reservoir water. Principal location of electrodes marked out.

spillway structure (Fig. 1). The left dam is 120 m and the right dam is 200 m long. Both dams have a maximum height of around 30 m in the central part of the river section and level out at the abutments. The dams are constructed as zoned embankments with a vertical low permeable central core of till surrounded by filter zones of sand on each side and coarse rockfill (Fig. 2). The dams operate under steady state seepage. The till core serves to minimize seepage and the rockfill serves to stabilise the dam. The main functions of the filter are to drain seepage water passing the core and to protect the fine material in the core from being washed out in the coarse rockfill. Water level variations are less than 0.8 m (+291.2–+292.0 m a.s.l.), which gives ideal conditions for the measurements as water level changes add difficulties in the interpretation of monitoring data. Except for the resistivity system, the dams were until 2003 rather sparsely monitored with a few piezometers and a drainage system measuring leakage from the left dam. In 2004 the drainage system has been updated and new piezometers have been installed. Furthermore, starting in 2004 a seven meter wide zone of very coarse rockfill is being placed on the full height of the downstream slope.

The dam is classified into the highest consequence class in RIDAS, the Swedish guidelines for dam safety. A sinkhole was observed in 1985, located close to the intake structure on the left dam. The sinkhole at Hällby was repaired by grouting. After additional drilling on the right dam it was decided to grout the area close to the spillway (Bronner et al., 1988). Nilsson et al. (1999) pointed at a link between inadequate filter design and development of sinkholes on Swedish embankment dams. Material from the core is transported with the seepage flow into the downstream filter (internal erosion). As this increases it develops towards the upstream side. Further on a material deficit in the upstream filter occurs, which may lead to an internal structural collapse, which eventually can be recognised at the top of the dam. In general this is a slow development, and in some cases it heals by itself. Nevertheless, it may put the safety of the dam at stake and it is therefore crucial to discover such progress as early as possible.

The installation comprises full instrumentation for resistivity measurements. The system is based on the ABEM Lund Imaging System, with modifications for automatic monitoring needs including lightning protection. A PC controls the data acquisition, with a modem for remote control and data transfer. Five cables with permanently installed electrodes are situated on the reservoir bottom along the upstream slope of the dam (left and right), buried along the dam crest (left and right) and along the downstream toe (right only).

In total 102 electrodes are installed on the dam, of which 43 on the crest and 21 on the downstream toe. Stainless steel plates were used as electrodes on land. The remaining 38 electrodes were installed in the reservoir on the dam upstream face, using stainless steel ring electrodes. The distance between each electrode is seven meters. The installations at Hällby have been described more thoroughly in previous reports (Johansson et al., 2000). The monitoring system has performed quite well with only three longer breaks, 2–4 months each during the winters of 2000 and 2002 and the summer of 2004, since the start 1996. Only in one of the cases the break was caused by malfunction of a component in the resistivity monitoring equipment.

3. Method

Data quality has been assessed by comparing reciprocal Wenner–Schlumberger measurements, and has been found to be unsatisfying for some of the layouts. Particularly, data from the right dam crest, where a thermal insulation layer is present between the electrodes and the dam core, causing high electrode contact resistances and troublesome noise levels (Johansson et al., 2000). The other two on-shore layouts (left crest and right downstream toe) also suffer from high contact resistances, especially in winter, but have lower noise levels. The somewhat questionable data quality for the on-shore layouts demands special treatment and for this reason de-spiking and low-pass filtering methods have been implemented in the data processing routines to filter the data before an inverse modelling is carried out. Filter parameters were adjusted to remove peaks successfully without disturbing the natural variations.

The results shown in this paper was processed with a low-pass filtering method using an IIR (infinite impulse response) routine, based on the following formula:

$$\rho^{\mathrm{f}}_{n+1} = \frac{\rho^{\mathrm{f}}_{n} + f\,\rho^{\mathrm{m}}_{n+1}}{1+f}, \tag{1}$$

where $\rho^{f}_{n+1}$and ρ^{f}_{n} are the filtered values from time step $(n+1)$ and n respectively, and ρ^{m}_{n+1} represents measured raw data for time step $(n+1)$. The factor f may be for example 0.2. In addition, a maximum threshold for the impact of a new data (e.g. 40% of the present filtered value) acts as a de-spiking filter. In order not to shift the filtered data series towards higher dates the filter is run forwards and backwards, and the average taken as the filtered data.

The success of this approach is dependent on good start values at each end of the time series, if a heavily distorted start value is used it will shift a large portion of the filtered series. To avoid this, an approach that can be described as a median–mean is adopted to find suitable start values, in which the initial data points (from e.g. a couple of weeks) are sorted and a mean is taken after excluding a number of data points in each end of the sorted table. However, if a longer break in the data series should occur particular care needs to be taken to assure a good filter function.

Combined automatic routines for handling long monitoring periods, filtering data, inverting data and finally present some statistical parameters for the whole period have been developed. Prototype software has been developed that automatically goes through a five step procedure; data extraction from archives, data filtering, calculation of reference data sets, inverse numerical modelling and finally calculation of statistical parameters and data presentation.

Data sets were inverted using the software Res2dinv version 3.54r for Win XP. The data from 2-D electrical imaging surveys is commonly inverted with a smoothness-constrained least-squares optimization method (deGroot-Hedlin and Constable, 1990). The subsurface is divided into a large number of rectangular cells, and the optimization method attempts to determine the resistivity of the cells that minimizes the difference between the calculated and measured apparent values subject to certain constraints (Loke et al., 2003). The equation used by this method is as follows.

$$\left(\mathbf{J}_i^{\mathrm{T}}\mathbf{R}_{\mathrm{d}}\mathbf{J}_i + \lambda_i\mathbf{W}^{\mathrm{T}}\mathbf{R}_{\mathrm{m}}\mathbf{W}\right)\Delta\boldsymbol{r}_i = \mathbf{J}_i^{\mathrm{T}}\mathbf{R}_{\mathrm{d}}\boldsymbol{g}_i - \lambda_i\mathbf{W}^{\mathrm{T}}\mathbf{R}_{\mathrm{m}}\mathbf{W}\boldsymbol{r}_{i-1}, \tag{2}$$

where $\boldsymbol{g}_i$ is the data misfit vector containing the difference between the logarithms of the measured and calculated apparent resistivity values, $\Delta\boldsymbol{r}_i$ is the change in the model parameters for the ith iteration and $\boldsymbol{r}_{i-1}$ is the model parameters (the logarithm of the model resistivity values) vector for the previous iteration. $\mathbf{J}$ is the Jacobian matrix of partial derivatives and $\mathbf{W}$ is a first-order roughness filter (deGroot-Hedlin and Constable, 1990). The damping factor λ determines the relative importance given to minimizing the model roughness and data misfit. $\mathbf{R}_{\mathrm{d}}$ and $\mathbf{R}_{\mathrm{m}}$ are weighting matrices introduced to modify the weights given to the different elements of the data misfit and model roughness vectors. By adjusting the form of these weighting matrices, the L_1 or L_2 norms can be used in the data misfit and model roughness minimizations. A more detailed description of the inversion method is given in Farquharson and Oldenburg (1998).

Loke et al. (2003) describes the use of the L_1 and L_2 optimization norms in 2-D resistivity inversion. The L_1-norm optimisation was chosen for all inversions in this paper. Apart from being more robust to noisy data, it tends to produce models with regions that are more blocky and separated by sharper boundaries. The latter factor is

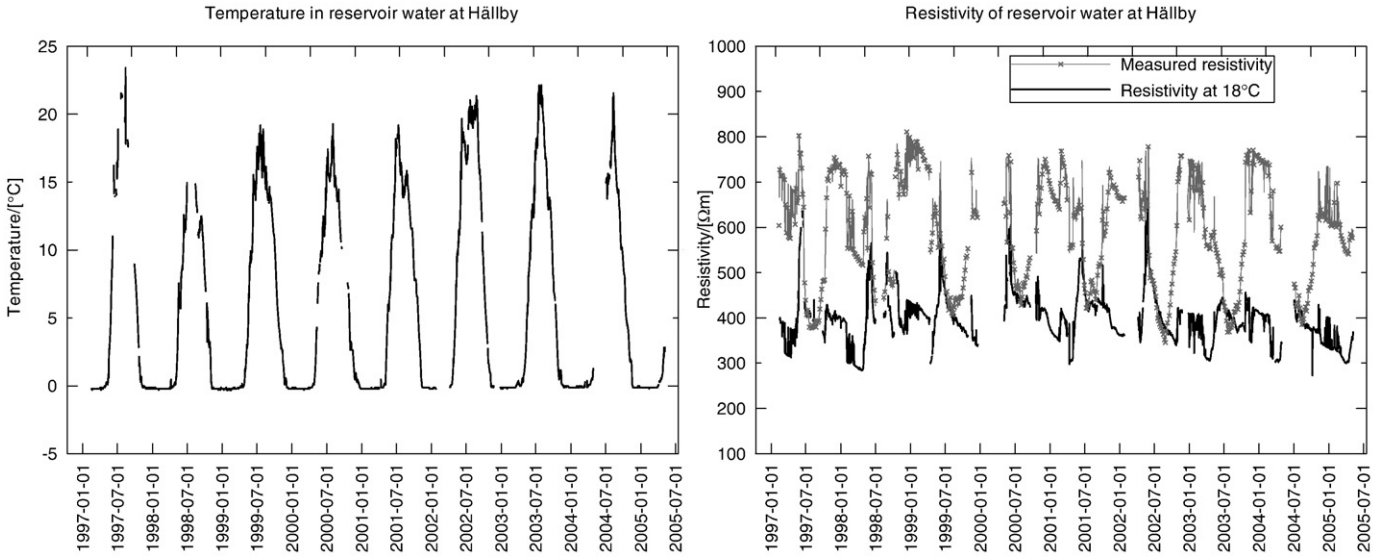

Fig. 3. Temperature in the reservoir water (left). Measured resistivity and normalised resistivity at 18 °C (right).

probably more consistent relating to measurements on a zoned embankment, where large resistivity contrast is expected between different materials, i.e. between the fine-grained core and the fresh igneous rock of its foundation.

Time-lapse inversion means that two data sets from different points of time are inverted together, where the first recorded data set would normally be regarded as a reference. In time-lapse inversion a smoothness constraint is applied not only on the spatial variation but also on the temporal variation between the data sets. This approach has been shown to focus the difference between the data sets on the actual change in the model and suppress artefacts due to the resistivity structure (Loke, 2001). It takes into account the fact that in many situations the changes in the resistivity occur in a limited section of the subsurface while the rest of the subsurface has much smaller changes. Thus the optimisation Eq. (2) is modified such that it also minimizes the difference in the logarithm of the model resistivity values of the later time data set and the initial time data set. The modified equation used is given by

$$\begin{aligned}&\left(\mathbf{J}_i^{\mathrm{T}}\mathbf{R}_{\mathrm{d}}\mathbf{J}_i+\lambda_i\mathbf{W}^{\mathrm{T}}\mathbf{R}_{\mathrm{m}}\mathbf{W}\right)\delta\boldsymbol{m}_i^k\\&\quad=\mathbf{J}_i^{\mathrm{T}}\mathbf{R}_{\mathrm{d}}\boldsymbol{g}_i-\lambda_i\mathbf{W}^{\mathrm{T}}\mathbf{R}_{\mathrm{m}}\mathbf{W}\boldsymbol{m}_{i-1}^k-\beta_i\lambda_i\mathbf{V}^{\mathrm{T}}\mathbf{R}_{\mathrm{t}}\mathbf{V}\left(\boldsymbol{m}_{i-1}^k-\boldsymbol{m}_{i-1}^0\right),\end{aligned}\tag{3}$$

where $\boldsymbol{m}_{i-1}^0$ and $\boldsymbol{m}_{i-1}^k$ are the model parameter vectors for the initial data set and the kth time data set. The additional term, $\beta_i\lambda_i\mathbf{V}^{\mathrm{T}}\mathbf{R}_{\mathrm{t}}\mathbf{V}(\boldsymbol{m}_{i-1}^k-\boldsymbol{m}_{i-1}^0)$, on the right-hand side of the above equation constrains the change in the model for the kth time data set such that the difference between the model resistivity values for this data set and the model for the initial time data set (which serves as a reference model) is also minimized. β is the relative weight given to this cross-model constraint and $\mathbf{V}$ is the cross-model weighting matrix that determines the characteristic that we wish to introduce in the differences in the model resistivity values. For example, if a simple damped or Marquardt (Lines and Treitel, 1984) cross-model constraint is used, then $\mathbf{V}$ is the identity matrix $\mathbf{I}$. $\mathbf{R}_{\mathrm{t}}$ is the weighting matrix that modifies the weights given to the different elements of the model difference vector such that the L_1 or L_2 norm can be used (Farquharson and Oldenburg, 1998). If it is known that the time changes in the model resistivity values vary spatially in a smooth manner (for example a chemical plume that spreads by diffusion), then the L_2 norm constraint can be used. Alternatively, if it is known that the changes are expected to exhibit a blocky character, the L_1 norm constraint is more appropriate.

We tested inverting the filtered data sets in various ways without time-lapse constrains, as well as with different reference data sets. Time-lapse inversion with a sliding damped reference value, which was filtered with a stronger damping than the data set itself to avoid noise contamination of the reference data sets, turned out to give best results in terms of extracting model series with credible temporal variation. Using an all time median as constraining data set for the time-lapse inversion tends to damp out variation that appears to contain useful information, since the inversion in that case cannot account properly for the high contrast in near surface resistivity with strong seasonal variation caused by for example freezing of the ground. The inverted data presented here was processed using the L_1-norm and a sliding damped reference data set with a time-lapse damping factor (β) of 1.0.

4. Results

The temperature and resistivity of the water in the reservoir have been measured since the start of the monitoring program (Fig. 3). The pattern of the temperature variation is sinusoidal over the year but with a clear cut over the lower part of the curve at 0 °C. The resistivity curve (Fig. 3) shows similar characteristics as it is depending heavily on temperature, but the higher winter resistivity is clearly affected by differences in ion content as well, probably due to seasonally varying inflow of groundwater to the river. Absolute values ranging from 400–700 Ω m represent very resistive water which is common in Scandinavian fresh water (SLU, 2008). Normalising resistivity data with respect to temperature using Eq. (4) (e.g. Ward, 1990) removes much of the seasonal variations. National environmental monitoring data from Sollefteå, situated approximately 100 km downstream Hällby dam, indicate resistivities (normalised to 18 °C) between 310 Ω m and 430 Ω m in the actual period (SLU, 2008). This agrees well with the temperature normalised data from the dam.

$$\rho_t=\frac{\rho_{18}}{(1+\alpha(T-18))},\alpha=0.25,\tag{4}$$

In early summer, however, a remaining resistivity peak can be observed in the adjusted data. Most likely this peak is related to snowmelt, which, for the geographic location, occurs in May. Nevertheless, it is obvious that, except for freezing of the ground in the

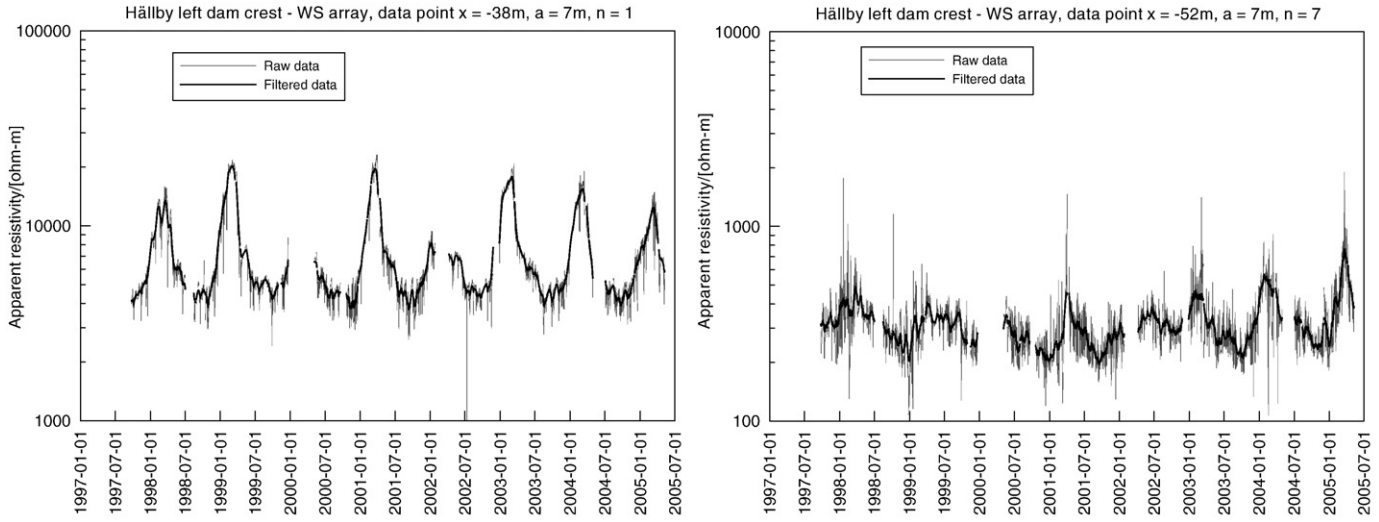

Fig. 4. Raw data (apparent resistivities) and filtered data from two specific measurement configurations on Hällby left dam crest. Left: Wenner–Schlumberger array with midpoint at chainage −38 m, a-spacing 7 m and *n*-factor = 1. Right: Wenner–Schlumberger array with midpoint at chainage −52 m, a-spacing 7 m and *n*-factor = 7.

shallow depths, the temperature of the water is the main reason for seasonal resistivity variation both in the reservoir and inside the dam.

Fig. 4 gives two examples of raw data (apparent resistivity) over time from the left dam crest layout; the first one, to the left, is from a reasonably good data measurement configuration with low noise levels whereas the second one, to the right, is an example of really poor data quality. Data from the downstream layout is similar or slightly better. The same type of presentation for the offshore layouts demonstrates that, in opposite to some of the on-shore measurements, the data quality is excellent in this case. This is due to the fact that the electrodes are placed under water, which results in excellent grounding conditions. The filter applied on the land data was used here as well and it successfully removes or smoothens out the rather few existing bad data points without affecting the natural variations (Fig. 5).

One part of the continuous evaluation from the monitoring program is to present the median inverted model section and the distribution of the relative variation (Fig. 6). The relative variation is a simple statistical measure that serves well with the intention of analysing size of variation in different areas of the dam. It is calculated as follows.

$$\text{Relative Variation} = (\rho_{\max} - \rho_{\min})/\rho_{\text{median}}, \quad (5)$$

The dam crest electrodes are installed 1 m below the crest (+293.5 m). One model is generated for every 7-day interval over the whole monitoring period. The median inverted model section is the median of all those models and represents average conditions for the dam but does not give us much information besides that. The relative variation is a very rough statistical parameter, but nevertheless it is valuable for interpretation and gives an overview of the seasonal variation in the dam. The variation is high close to the crest, which is explained by extremely high winter resistivities due to ground freezing. The high variation at the bottom is more remarkable. At weaker more permeable zones in the dam core, the impact from the seasonal resistivity variation in the reservoir will lead to larger variations caused by significant seepage. Therefore, high variations at large depth should be a seen as a warning. In addition the high

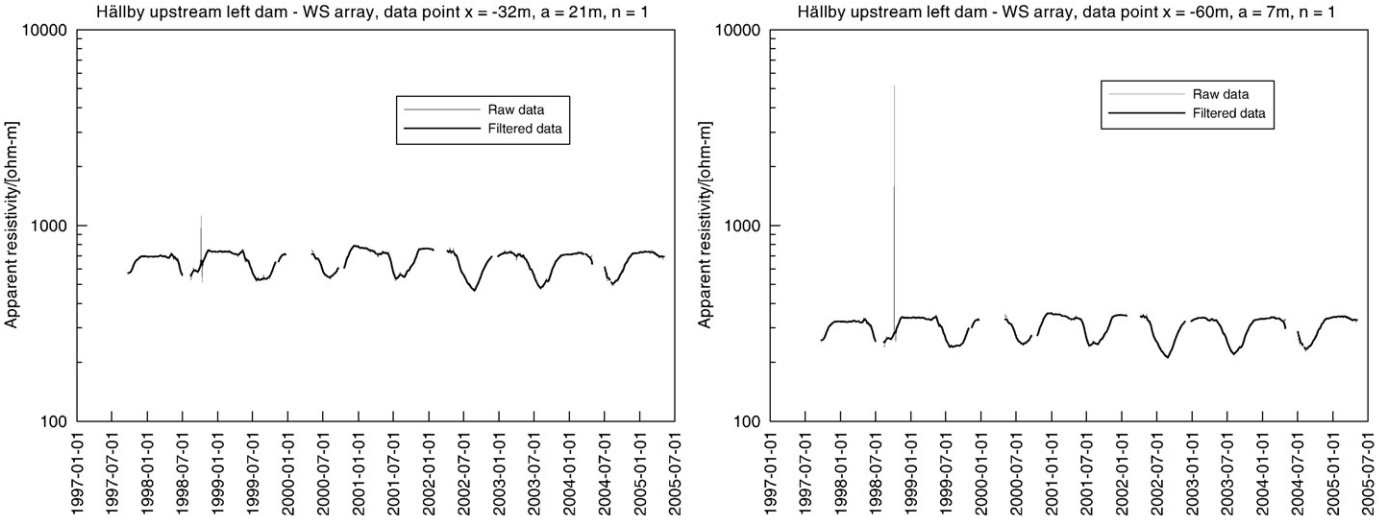

Fig. 5. Raw data and filtered data between 1997-09-24 and 2005-05-08 from two specific measurement configurations on the layout along the upstream side of Hällby left dam. Left: Wenner–Schlumberger array with midpoint at chainage −32 m, a-spacing 21 m and *n*-factor = 1. Right: Wenner–Schlumberger array with midpoint at chainage −60 m, a-spacing 7 m and *n*-factor = 1.

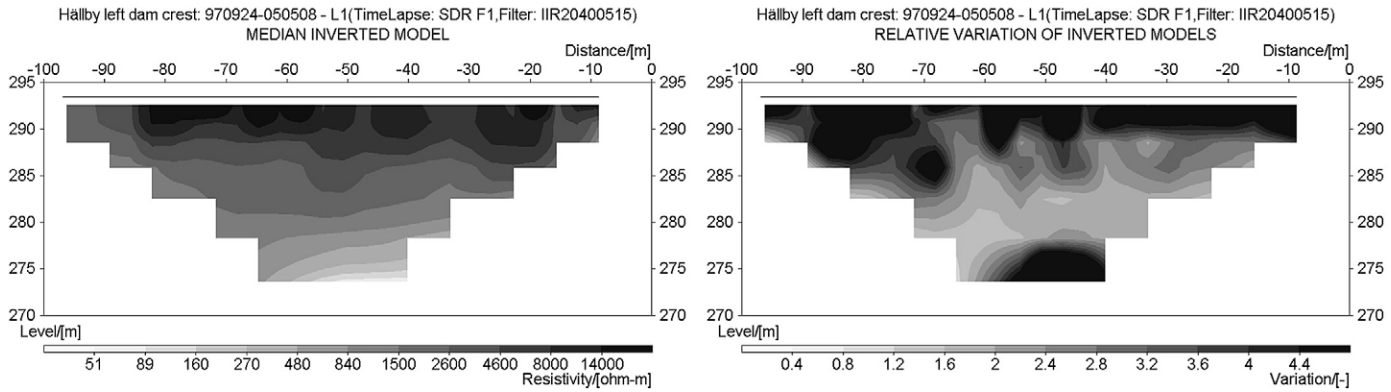

Fig. 6. Median inverted resistivity distribution (left) and its relative variation (right) at Hällby left dam crest between 1997-09-24 and 2005-05-08.

variation at the bottom of the dam has spread from right to left over the last two to three years and the area at the same depth at chainage −10 m (chainage is used to represent a certain length mark along the dam) to chainage −20 m is a known problem area from the past.

However, the complete model section serves only as an overall inspection and more detailed examinations should also be carried out. One example of such is to analyse the change in resistivity over time in a certain point of the model section. In Fig. 7 selected depths at chainages −61.25 m and −43.75 m are given in this form.

Chainage −61.25 m exhibits the kind of appearance that could be suspected and may serve as a reference for a healthy dam based on experiences from temperature measurements in similar dams (Johansson, 1997); resistivity values decreases with depth, and so does the variations (amplitudes). Variations on different depths are in a similar phase but may be slightly delayed with increasing depth. The shallower parts of the embankment are more resistive, and might also get influenced by freezing during winter. Furthermore, the amplitude of the variation becomes lower at larger depths. This is a quite typical appearance for most of the examined parts of the dam and consistent with theory as the impact from seasonal temperature variation in the reservoir or in the air should decrease with depth for a healthy dam. In addition, slight phase shifts might be identified when comparing variations at different depths, as the seepage path and thereby also the time delay is longer at larger depths.

As the section in Fig. 6 implies, there is a difference in size of the variation at large depths between chainage −61.25 m and −43.75 m. This higher variation is clearly visible for the largest model depth in the time series of chainage −43.75 m (Fig. 7, lower diagram). Furthermore, a tendency of a long term increase in resistivity is also evident for the largest depth. As the resistivity increases, due to material change in the soil, the variation also seem to increase, which could be interpreted as increasing seepage as a result of internal erosion. Small phase shifts might be observed, but these are not clear enough to draw any evident conclusions.

To further evaluate what is happening in this area data from other measurement arrays have been analysed. Pole–dipole measurements started in 1999 as a complement to the Wenner–Schlumberger setup mainly because of the possibilities to map larger depths and get better resolution towards the ends of the model. However, pole–dipole measurements are more difficult to evaluate, due to inversion complications arising from high contrasts resulting from conductive sheet-pile in the dam core at the connection to the concrete structure in combination with higher noise levels. Some indications of resistivities increasing in time can be noticed in the same area as where the Wenner–Schlumberger readings showed an increase, which might be seen in the time series of chainage −40.25 m at depths 9.0 m and 16.8 m (Fig. 8). An interesting observation from the pole–dipole data is that at depth 22.2 m the resistivities are already much higher indicating that the high resistivity of the foundation is observed. The explanation of this depth distortion is likely to originate from geometrical effects when inverting two-dimensional resistivity data over an embankment geometry (Sjödahl et al., 2006).

Unfortunately no installation of electrodes was done along the downstream toe of the left dam due to difficulties to access that area. The main idea behind monitoring the downstream toe is to be able to check for leakage in the foundation. However, even though downstream measurement is less informative about the situation in the dam, it is possible that they also could be used for as an aid when interpreting observations on the other layouts to help getting an overall picture of the situation in the whole dam. Downstream measurements on the right dam uncover nothing unexpected. A representative example from chainage +50.75 m shows high seasonal variations at shallow depths and low variations on large depth (Fig. 9). Measurement ended in early summer 2004 on the downstream layout due to upgrading works on the dam. A new cable and electrodes have been installed but data is still analysed separately. In this case the seepage regime is not expected to enhance the variation as much and local seasonal air temperature is likely to have an effect only to a few metres depth at most in this kind of material.

The combined automatic routines for filtering and inverting data have been further developed by adding daily reservoir levels and water resistivities in the inversion scheme. The electrodes in the layout along the upstream side of the left dam are placed on the slope of the dam on 7–9 m water depth (+284.0 m ± 1 m), and the resistivity distribution given by the upstream layout is rather homogenous with a large zone with higher resistivities in the right part (Fig. 10). The yearly variations are generally much lower than for the crest throughout the section, but for a zone around chainage −20 m to chainage −40 m the variations are significantly higher down to 10 m depths. The upstream electrode layout follows the slope of the dam, which is slightly curved towards the right end where the dam, at chainage 0 m, connects to a large concrete structure hosting the power plant intake. Therefore the dam length marks are only approximate for the upstream layout. In addition, the bending of the line may lead to distortions in resistivity data but the variations, which are of higher interest, should be much less affected.

In the time series of inverted data from the upstream layout the seasonal variations are generally small (Fig. 11). This seems reasonable, as temperature variations on 7–9 m water depth are small in this climate. Data from the above mentioned zone in the right part shows signs of a larger and a much more messy variation (Fig. 11). This could be a sign of higher seepage. It should be noted that the variations become lower at the very far right end making it implausible that the higher variations originate from disturbances related to inflow of water to the power station. In opposite to the crest measurements, there are no signs of long term increase or decrease in resistivity for

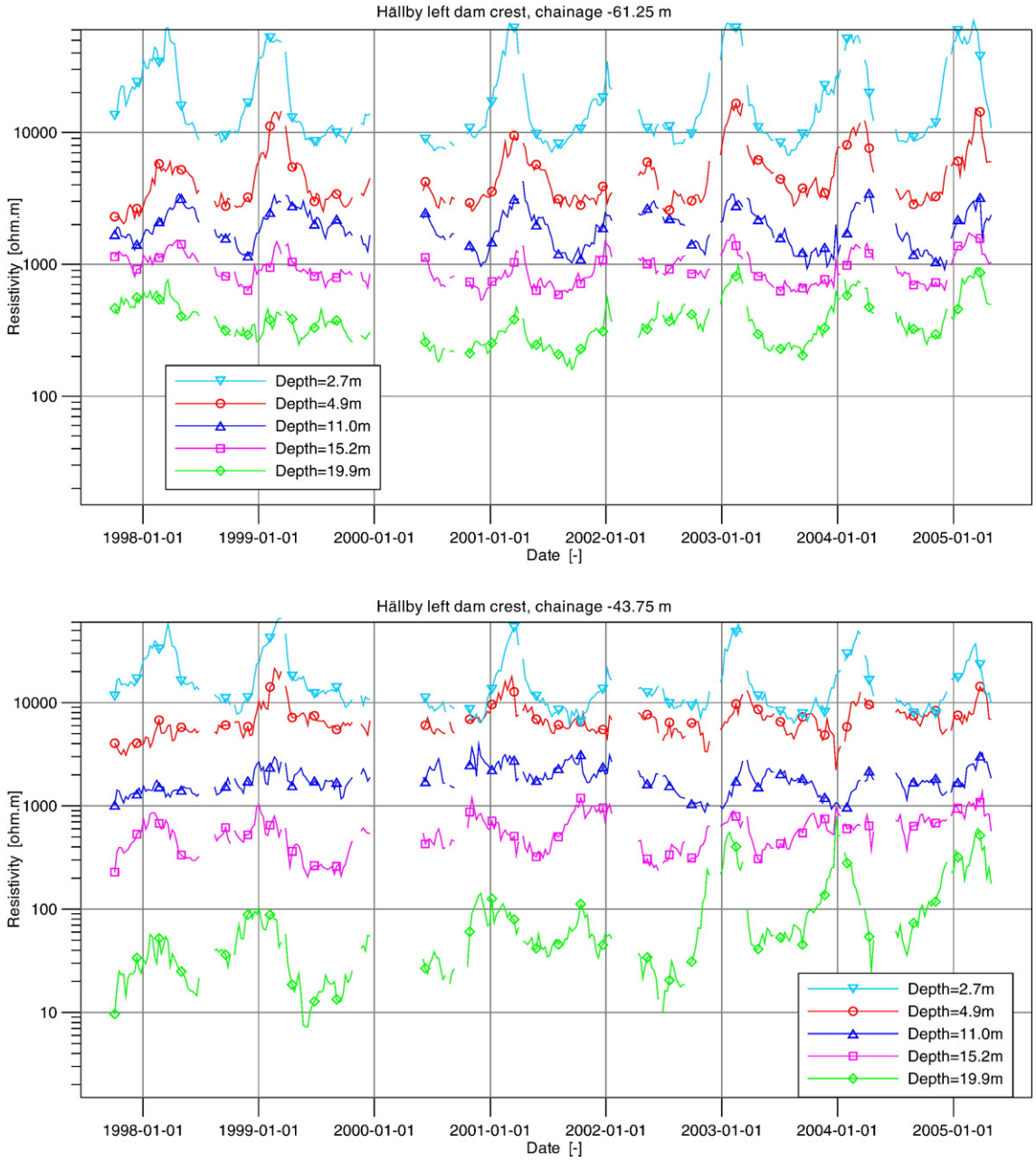

Fig. 7. Examples of time series of inverted resistivity data at five different depths from two different locations on Hällby left dam; Chainage −61.25 m (above) and chainage −43.75 m (below).

any of the upstream measurements. As long term changes are associated with changes in material properties, we do not expect to find such changes, because internal erosion or any other phenomena affecting the material properties are unlikely to occur in the upstream support rockfill.

5. Discussion and conclusions

In a healthy dam with constant material properties over time, the measured resistivity can be considered as a function of the seepage flow only. The variations of temperature and TDS in the reservoir create resistivity variation inside the dam as the water seeps through the dam body. Temperature and total dissolved solids, TDS, are the main elements governing the resistivity of the water. Compensating for temperature by calculating the resistivity at 18 °C gives the impression that most of the variation results from temperature changes, but TDS variations are significant. High resistive peaks caused by low TDS may be identified during the snowmelt period.

Assuming TDS to be constant in the water as it seeps through the dam, the seepage can be estimated using temperature evaluation methods involving analysing lag-times and amplitudes, or by using TDS pulses as a natural tracer (Johansson, 1997). These methods use the combined theories of transports of heat and flow to compare the seasonal resistivity variation of the reservoir water and inside the dam to estimate the leakage through the dam.

In the evaluation of repeated measurements, the focus is on discovering and locating zones with long term changes in trends or with abnormal variations in time, within the dam core. The method of time-lapse inversion has been recognised as a promising way to

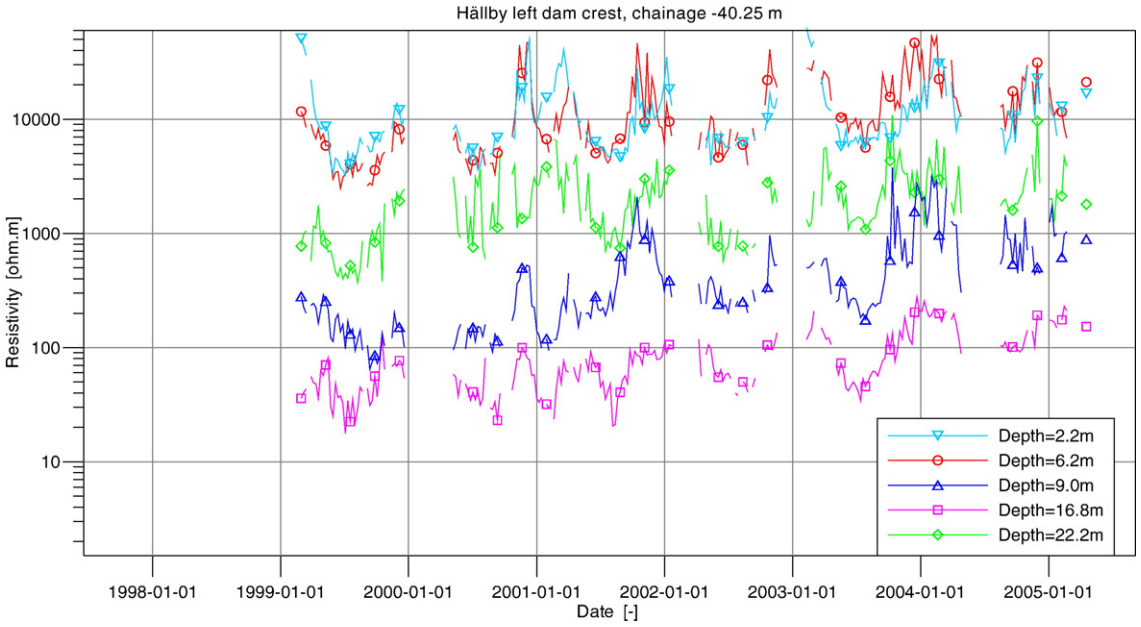

Fig. 8. Examples of time series of inverted resistivity pole–dipole data at five different depths from Hällby left dam; Chainage −40.25 m.

analyse these variations, which gave better results than inverting the data sets separately. Less consideration is given to absolute values as modelling studies of resistivity distribution on embankment geometries have shown that 3D effects are significant and that, for typical Swedish designs, the actual measurements with layouts along the dam crest may give readings several times higher than the resistivity of the core (Sjödahl et al., 2006). The same modeling study also showed that the layout along the crest is the most promising for locating changes in the dam core.

In a dam where internal erosion occurs, the fines in the core are being washed out and except for disturbances in the seasonal resistivity variation, i.e. increasing amplitudes and possible phase shifts, a long term trend should be possible to detect. Most Swedish dams, being constructed with a till core, are expected to show a raise in resistivity if such a scenario should occur given the generally very low ion content of the river waters. Laboratory tests on similar tills used in sealing layers for waste deposits have shown that the resistivity may rise ten times or more due to removal of fines under water saturated conditions (Bergström, 1998). However, this is to some extent counteracted as internal erosion increases porosity, affecting the resistivity in the opposite direction even though the water resistivity is very high. A soil may respond to increased porosity by either increasing or decreasing resistivity depending on the strength of surface conduction in the soil (Revil et al., 1998). The left dam at Hällby has had problems with internal erosion leading to sinkholes. Increasing pore water pressures have also been observed in the left dam support fill, which is one of the reasons for a recent decision on reinforcing the downstream support fill. Increasing resistivities and increasing variation has been observed, by the crest measurements, in a zone of the left dam next to the zone that had

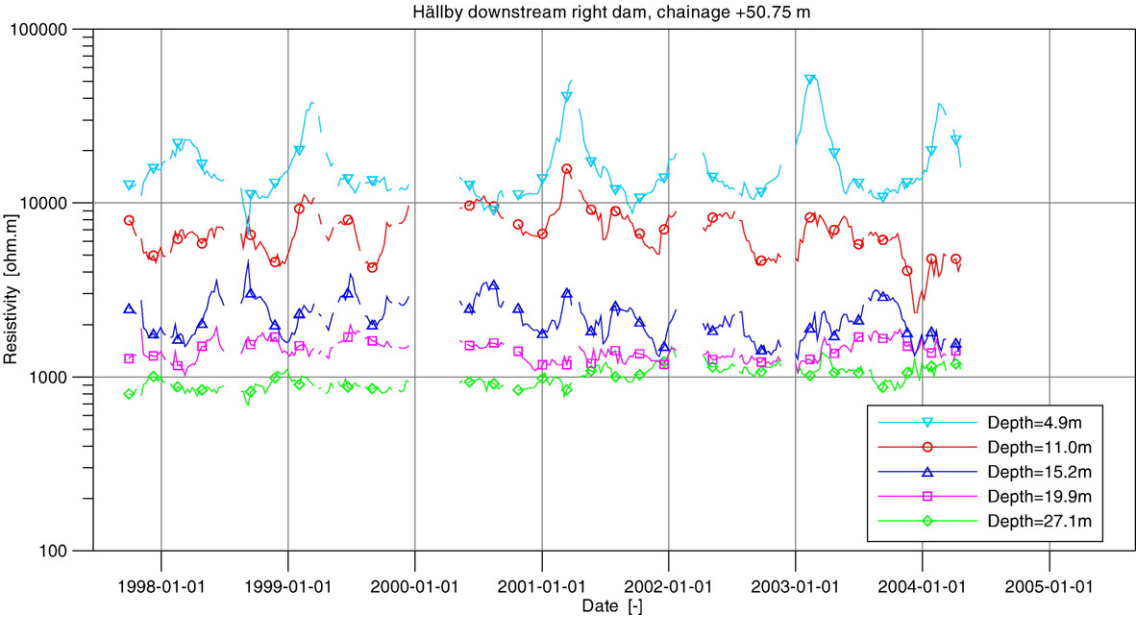

Fig. 9. Examples of time series of inverted resistivity data at five different depths from downstream Hällby right dam; Chainage +50.75 m.

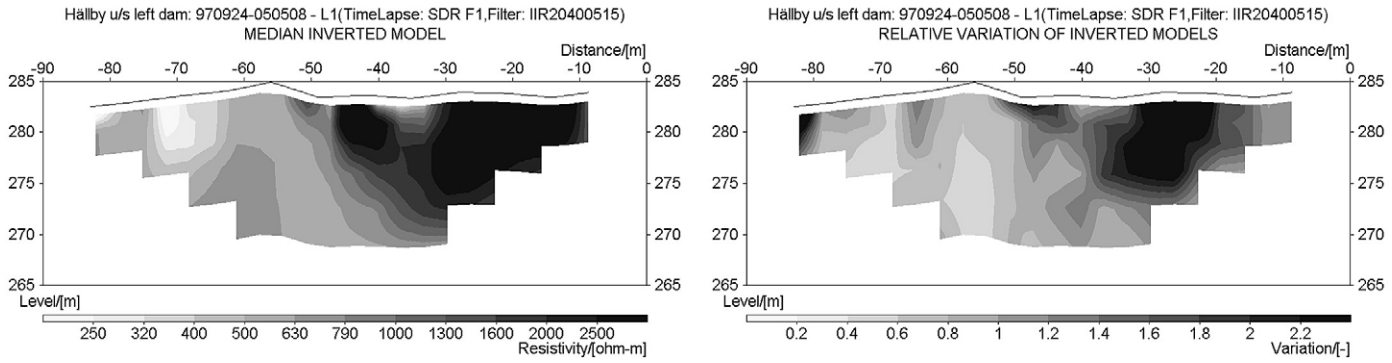

Fig. 10. Median inverted resistivity distribution (left) and its relative variation (right) upstream Hällby left dam between 1997-09-24 and 2005-05-08 (approx. length marks).

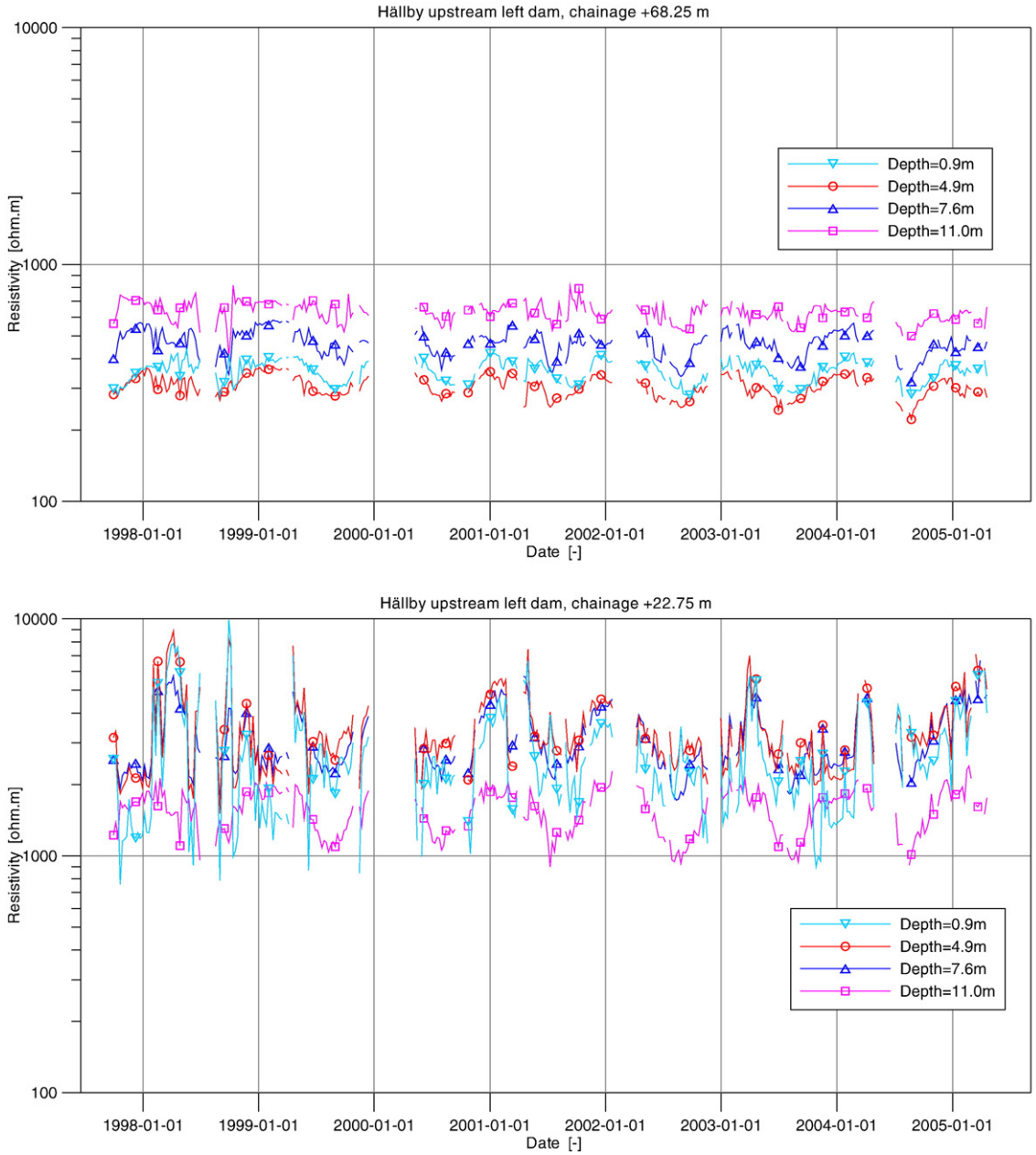

Fig. 11. Examples of time series of inverted resistivity data at four different depths from two different locations upstream Hällby left dam; Chainage −68.25 m (above) and chainage −22.75 m (below) (approx. length marks).

prior reports of sinkholes. This might be an indication of internal erosion.

The layout along the downstream toe may be able to detect seepage zones in the foundation and may help interpret data from inside the dam. However, we have not been able to support this with monitoring data, as the downstream area of the left dam was not accessible for electrode installations. Results from the right downstream side show stable conditions with high near surface seasonal variation decreasing with depth.

Measurements along the upstream side of the dam can be easier to carry out in practise, provided the electrode layout can be laid out and positioned without complications on the upstream side. Monitoring installations inside the reservoir also avoid problems associated with high contact resistances and freezing, if the variation in reservoir level is limited enough so that the electrode layout is never exposed. At Hällby, the results from the offshore measurements point in the same direction as the crest measurements, but do not give the same amount of information, which makes them a compliment rather than a substitute.

Finally, electrode installations are important to ensure good data quality and electrode spacing should preferably be kept as small as possible, but even with quite noisy data and relatively few electrodes, the monitoring results from Hällby have shown that accurate handling of the time series with filtering and inversion techniques may still lead to very useful information. At Sädva, the other Swedish dam site with an installed resistivity monitoring system, electrode spacing is less than half of the one at Hällby and data quality noticeably better. Detailed analysis from resistivity monitoring data from Sädva is in progress.

Acknowledgements

The work presented here was supported by research grants from Elforsk, Svenska Kraftnät, DSIG (Dam Safety Interest Group) and Vinnova/VBT-konsortiet. The staff at Hällby dam has given valuable support.

References

Aaltonen, J., 2001. Seasonal resistivity variations in some different Swedish soils. European Journal of Engineering and Environmental Geophysics 6, 33–45.

Aina, A., Olurunfemi, M.O., Ojo, J.S., 1996. An integration of aeromagnetic and electrical resistivity methods in dam site investigation. Geophysics 61, 349–356.

Aristodemou, E., Thomas-Betts, A., 2000. DC resistivity and induced polarisation investigations at a waste disposal site and its environments. Journal of Applied Geophysics 44, 275–302.

Barker, R.D., Moore, J., 1998. The application of time-lapse electrical tomography in groundwater studies. The Leading Edge 17, 1454–1458.

Batayneh, A.T., Abdallah, S.A.Z., Abdelruhman, A.A., 2001. Geophysical investigations for the location of a proposed dam in Al Bishriyya (Al Aritayn) area, northeast Badia of Jordan. Environmental Geology 40, 918–922.

Bergström, J., 1998. Geophysical Methods for Investigating and Monitoring the Integrity of Sealing Layers on Mining Waste Deposits. Licentiate Thesis, Luleå University of Technology, Luleå, Sweden, ISSN: 1402-1757 ISRN: LTU-LIC — 98/24 — SE, 77p.

Bronner, N., Fagerström, H., Stille, H., 1988. Bedrock cracks as a possible cause of leakage in two Swedish dams. Procs. International Commission on Large Dams (ICOLD), 16th Congress, San Fransisco. Q.61, R.55.

Buselli, G., Lu, K., 2001. Groundwater contamination monitoring with multichannel electrical and electromagnetic methods. Journal of Applied Geophysics 48, 11–23.

Chambers, J.E., Loke, M.H., Ogilvy, R.D., Meldrum, P.I., 2004. Noninvasive monitoring of DNAPL migration through a saturated porous medium using electrical impedance tomography. Journal of Contaminant Hydrology 68, 1–22.

Cho, I.-K., Yeom, J.-Y., 2007. Crossline resistivity tomography for the delineation of anomalous seepage pathways in an embankment dam. Geophysics 72, 31–38.

Cuthbert, M.O., Russell, E.J.F., Barker, R.D., Mackay, R., 2004. The effect of seasonal temperature variations on the resistivity of glacial till. Procs. 10th EEGS-Meeting, Utrecht, The Netherlands, 6–9 September. 4 pp.

Dahlin, T., Sjödahl, P., Friborg, J., Johansson, S., 2001. Resistivity and SP surveying and monitoring at the Sädva embankment dam, Sweden. Procs. 5th European ICOLD Symposium, 25–27 June 2001, Geiranger, Norway. Balkema, Lisse, pp. 107–113.

deGroot-Hedlin, C., Constable, S., 1990. Occam's inversion to generate smooth, two-dimensional models from magnetotelluric data. Geophysics 55, 1613–1624.

Depountis, N., Harris, C., Davies, M.C.R., Koukis, G., Sabatakakis, N., 2005. Application of electrical imaging to leachate plume evolution studies under in-situ and model conditions. Environmental Geology 47, 907–914.

Farquharson, C.G., Oldenburg, D.W., 1998. Non-linear inversion using general measures of data misfit and model structure. Geophysical Journal International 134, 213–227.

French, H., Binley, A., 2004. Snowmelt infiltration: monitoring temporal and spatial variability using time-lapse electrical resistivity. Journal of Hydrology 297, 174–186.

Jackson, P.D., Nortmore, K.J., Meldrum, P.I., Gunn, D.A., Hallam, J.R., Wambura, J., Wangusi, B., Ogutu, G., 2002. Non-invasive moisture monitoring within an earth embankment — a precursor to failure. NDT&E International 35, 107–115.

Johansson, S., 1997. Seepage Monitoring in an Earth Embankment Dams. Doctoral Thesis, TRITA-AMI PHD 1014, ISBN 91-7170-792-1, Royal Institute of Technology, Stockholm.

Johansson, S., Dahlin, T., 1996. Seepage monitoring in an earth embankment dam by repeated resistivity measurements. European Journal of Engineering and Environmental Geophysics 1 (3), 229–247.

Johansson, S., Dahlin, T., 1998. Seepage monitoring in Hällby embankment dam by continuous resistivity measurements. Procs. 8th Congress of the International Ass. of Eng. Geology and the Environment, Vancouver, 21–25 September. 8 pp.

Johansson, S., Dahlin, T., Friborg, J., 2000. Seepage monitoring by resistivity and streaming potential measurements at Hällby embankment dam 1996–1999. Report 00:15. Elforsk, Stockholm. 47 p.

Kayabali, K., Yüksel, F.A., Yeken, T., 1998. Integrated use of hydrochemistry and resistivity methods in groundwater contamination caused by a recently closed solid waste site. Environmental Geology 36, 227–234.

LaBrecque, D.J., Ramirez, A.L., Daily, W.D., Binley, A.M., Schima, S.A., 1996. ERT monitoring of environmental remediation processes. Measurement Science & Technology 7, 375–383.

Lines, L.R., Treitel, S., 1984. Tutorial — a review of least-squares inversion and its application to geophysical problems. Geophysical Prospecting 32, 159–186.

Loke, M.H., 2001. Constrained time-lapse resistivity imaging inversion. Procs. SAGEEP 2001 (Symposium on the Application of Geophysics to Engineering and Environmental Problems). Denver, Colorado, March 4–7 2001.

Loke, M.H., Acworth, I., Dahlin, T., 2003. A comparison of smooth and blocky inversion methods in 2D electrical imaging surveys. Exploration Geophysics 34, 182–187.

Nilsson, Å., Ekström, I., Söder, C.-O., 1999. Inre erosion i svenska dammar. Elforsk report 99, 34 (in Swedish).

Osiensky, J.L., 1995. Time series electrical potential filed measurements for early detection of groundwater contamination. Journal of Environment Science and Health A30, 1601–1626.

Panthulu, T.V., Krishnaiah, C., Shirke, J.M., 2001. Detection of seepage paths in earth dams using self-potential and electrical resistivity methods. Engineering Geology 59, 281–295.

Rein, A., Hoffmann, R., Dietrich, P., 2004. Influence of natural time-dependent variations of electrical conductivity on DC resistivity measurements. Journal of Hydrology 285, 215–232.

Revil, A., Cathles, L.M., Losh, S., Nunn, J.A., 1998. Electrical conductivity in shaly sands with geophysical applications. Journal of Geophysical Research 103, 23925–23936.

Sjödahl, P., Dahlin, T., Zhou, B., 2006. 2.5D resistivity modeling of embankment dams to assess influence from geometry and material properties. Geophysics 71, 107–114.

SLU, 2008. Public Database of National Environmental Monitoring Data. Swedish University of Agriculture Sciences. www.ma.slu.se/ — 2008-06-10 (in Swedish).

Van Tuyen, D., Canh, T., Weller, A., 2000. Geophysical investigations of river dikes in Vietnam. European Journal of Environmental and Engineering Geophysics 4, 195–206.

Voronkov, O.K., Kagan, A.A., Krivonogova, N.F., Glagovsky, V.B., Prokopovich, V.S., 2004. Geophysical methods and identification of embankment dam parameters. Procs. 2nd International Conference on Site Characterization (ISC), Porto, Portugal, 19–22 September, pp. 593–599.

Ward, S.H., 1990. Resistivity and induced polarization methods. In: Ward, S. (Ed.), Investigations in Geophysics no. 5: Geotechnical and Environmental Geophysics, vol I. Society of Exploration Geophysicists, Tulsa, pp. 147–189.